In Situ Crystallization of Beta Zeolite Membranes and Their Permeation and Separation Properties

Vu A. Tuan, Shiguang Li, John L. Falconer,* and Richard D. Noble

Department of Chemical Engineering, University of Colorado, Boulder, Colorado 80309-0424

Received September 7, 2001
Revised Manuscript Received December 6, 2001

Zeolite membranes, which had high separation selectivities because of their molecular-sized pores, possess superior thermal, mechanical, and chemical properties. Most studies have focused on small-pore (0.42 nm, A-type)[1] and medium-pore (0.5−0.6 nm, MFI- and MEL-type) zeolite membranes,[2,3] and large-pore (0.65−0.74 nm, FAU- and MOR-type) zeolite membranes[4,5] have been less studied. Large-pore zeolite membranes have advantages for larger molecules, and they can be used as a host to immobilize large complexes. For example, a zeolite membrane, after modification with chiral *N*-3,5-dinitrobenzoyl-L-alanine, separated D/L-lactic acid enantiomers.[6] Among crystalline aluminosilicates, only beta zeolite has been shown to be a chiral zeolite.[7] Zeolite beta, a large-pore and high-silica zeolite with a typical Si/Al ratio of 10−25, possesses a three-dimensional 12-ring interconnected channel system with pore diameters of 0.71 × 0.73 nm.[8] Because beta zeolite is of potential industrial interest as a catalyst for fluid catalytic cracking,[9] hydrotreating,[10] dewaxing,[11] and alkylation,[12] significant effort has been devoted to synthesize and modify this type of zeolite. For example, Pt/H-beta was the best catalyst for total hydroisomerization of a gasoline fraction (*n*-C_5 to C_7) to obtain a product with high octane number without adding MTBE.[13] Therefore, if a beta zeolite continuous membrane can be prepared, it has potential for separations and catalytic membrane reactors owing to its unique pore structure and catalytic properties.

In the current study, Al-beta zeolite (Si/Al = 15) membranes were prepared by in situ crystallization onto tubular porous supports (α-Al_2O_3, 0.2-μm pores, US Filter; stainless steel, 0.5-μm pores, Mott Co.). About 1 cm on each end of the alumina supports was glazed, whereas nonporous stainless steel tubes were welded onto each end of the stainless steel supports prior to zeolite synthesis to provide a sealing surface for the O-rings used in membrane modules. Before synthesis, the supports were cleaned by brushing the inner surfaces of the tubes and then treating them in an ultrasonic bath that contained D.I. water. The support tubes were then boiled in D.I. water for 1 h and dried at 373 K under vacuum for 30 min. For zeolite synthesis, a mixture that contained 1.3 g of $NaAlO_2$ (53 wt % Al_2O_3, 43 wt % Na_2O) and 8 g of H_2O was stirred at room temperature until a clear solution was obtained. Then, 42.6 g of 40% TEAOH (tetraethylammonium hydroxide) in water was added. The TEAOH was used as the template. Next, 38.5 g of tetraethyl orthosilicate (TEOS) was added to the solution while stirring. The resulting mixture was heated at 323 K for 1 h while being stirred to remove ethanol that formed by TEOS hydrolysis. Note that ethanol must be completely removed to avoid formation of an amorphous material.

Before synthesis, one end of the support was wrapped with Teflon tape and plugged with a Teflon cap. The vertical tube was then filled with ≈2 mL of the synthesis gel; after sitting overnight, the tube was filled again with the synthesis gel because the first 2 mL soaked into the support. Crystallization without soaking the tube with synthesis gel led to the formation of amorphous material during the hydrothermal synthesis. The tube was placed vertically in a Teflon-lined autoclave, and zeolite synthesis was carried out at 393 K for 6 days. After growth of the first layer, the membranes were impermeable to nitrogen at room temperature, indicating that both intercrystalline and zeolite pores were filled with template molecules. The membranes were then calcined in air at 753 K for 8 h with heating and cooling rates of 0.011 and 0.015 K/s, respectively. Calcination removed the template from the zeolite pores. After calcination, however, the membrane contained intercrystalline pores, as indicated by high N_2 permeances (approximately 3×10^{-6} mol/m^2·s·Pa). These permeances were similar to those of the γ-alumina support, and the gas permeances of H_2, N_2, CH_4, and *i*-C_4 at room temperature were all similar. Five synthesis layers (each 6 days) were required to obtain continuous intergrown beta membranes, as indicated by N_2 permeances that were an order of magnitude lower (10^{-7} mol/m^2·s·Pa).

The powders collected from the bottom of membrane tubes were analyzed by X-ray diffraction (XRD) with a Scintag PAD-V diffractometer with Cu Kα radiation. All peaks for the powder collected when preparing a beta zeolite membrane on a stainless steel support (Figure 1a) match those reported by Robson[14] for beta zeolites with respect to the positions and intensities of

* To whom correspondence should be addressed. Phone: 303-492-8005. Fax: 303-492-4341. E-mail: john.falconer@colorado.edu.

(1) Kita, H.; Horii, K.; Ohtoshi, Y.; Tanaka, K.; Okamoto, K. *J. Mater. Sci. Lett.* **1995**, *14*, 206.
(2) Yan, Y.; Davis, M. E.; Gavalas, G. R. *Ind. Eng. Chem. Res.* **1995**, *34*, 1652.
(3) Tuan, V. A.; Li, S.; Noble, R. D.; Falconer, J. L. *Chem. Commun.* **2001**, 583.
(4) Nishiyama, N.; Ueyama, K.; Matsukata, M. *Chem. Commun.* **1995**, 1967.
(5) Li, S.; Tuan, V. A.; Falconer, J. L.; Noble, R. D. *Ind. Eng. Chem. Res.* **2001**, *40*, 1952.
(6) Szabo, L. P.; Lippai, E. H.; Handik, B.; Nagy, E.; Mizukami, F.; Shimizu, S.; Kiricsi, I.; Bodnar, J. *Hung. J. Ind. Chem.* **1998**, *26*, 147.
(7) Bruce, D. A.; Wilkinson, A. P.; White, M. G.; Bertrand. J. A. *J. Solid State Chem.* **1996**, *125*, 228.
(8) Baerlocher, Ch.; Meier, W. M.; Olson, D. H. *Atlas of zeolite framework types*; Elsevier: Amsterdam, 2001; p 77.
(9) Bonetto, L.; Camblor, M. A.; Corma, A.; Perezpariente, J. *Appl. Catal. A* **1992**, *82*, 37.
(10) Kiricsi, I.; Flego, C.; Pazzucoui, G.; Parker, W. O.; Millini, R.; Perego, C.; Bellussi, G. *J. Phys. Chem.* **1994**, *98*, 4627.
(11) Taylor, R. J.; Petty, R. H. *Appl. Catal.* **1994**, *119*, 121.
(12) Corma, A.; Martinez, A.; Arroyo, P. A.; Monteiro, J. I. F.; Sousa-Aguiar, E. F. *Appl. Catal. A* **1996**, *142*, 139.
(13) *Catalysis: An Integrated Approach*; van Santen, R. A., van leeuwen, P. W. N. M., Moulijn, J. A., Avenrill, B. A., Eds.; Studies in Surface Science and Catalysis 123; Elsevier: Amsterdam, 1999.

10.1021/cm010413e CCC: $22.00
Published on Web 01/18/2002

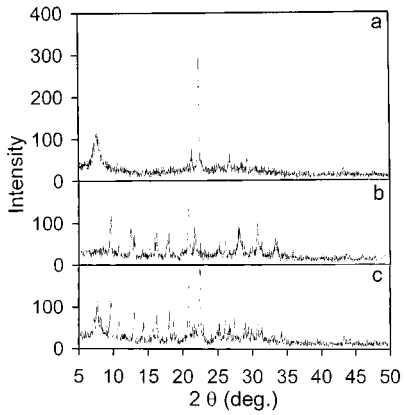

Figure 1. XRD spectra of powders collected when preparing beta membrane on (a) a stainless steel support, (b) an alumina support, and (c) a beta-zeolite-seeded alumina support.

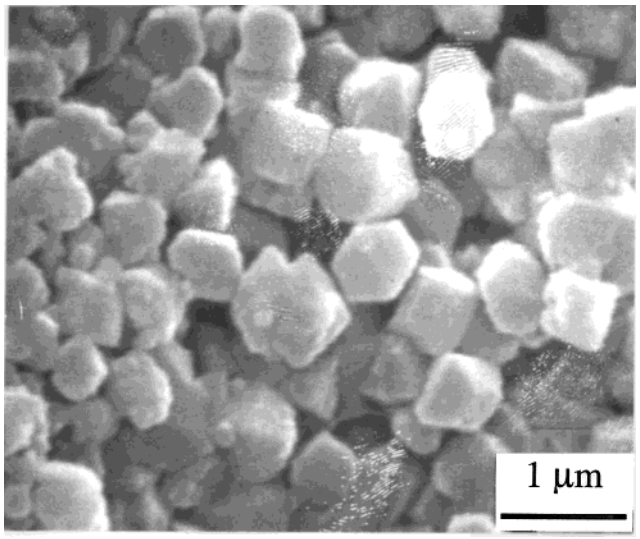

Figure 2. SEM of the surface of beta membrane M1 on a stainless steel support.

the reflections, and no additional peaks were observed. However, the XRD pattern of the powder collected when preparing beta membrane on an alumina support showed a structure that consisted of a mixture of ZSM-12 (MTW) and mordenite (MOR) phases (Figure 1b). The Si/Al ratios for ZSM-12 and mordenite are lower than the ratio for beta zeolite; apparently, some of the alumina support dissolved and substituted into the membrane framework, and this favored the formation of zeolites with lower Si/Al ratios. Interestingly, a different structure was observed when beta crystals were seeded onto the alumina support. The XRD pattern of powder collected from the bottom of beta-seeded alumina tube consisted of beta, ZSM-12, and mordenite (Figure 1c).

Two membranes, M1 and M2, were prepared on stainless steel by the same method, and they are expected to have the same properties. Membrane M1 was broken after pervaporation measurements and analyzed by SEM (ISI-SX-30). The surface of the membrane (Figure 2) has a continuous layer of intergrown crystals 0.4−0.7 μm in diameter. The stainless-steel-supported membrane was difficult to break for SEM analysis, but the zeolite layer appeared to be 40−50-μm thick. The high intensity of the XRD lines and the crystals shown in the SEM micrograph indicate a high degree of crystallinity of the beta membrane on the stainless steel support.

(14) Robson, H. *Verified Syntheses of Zeolitic Materials*; Elsevier: Amsterdam, 2001; p 117.

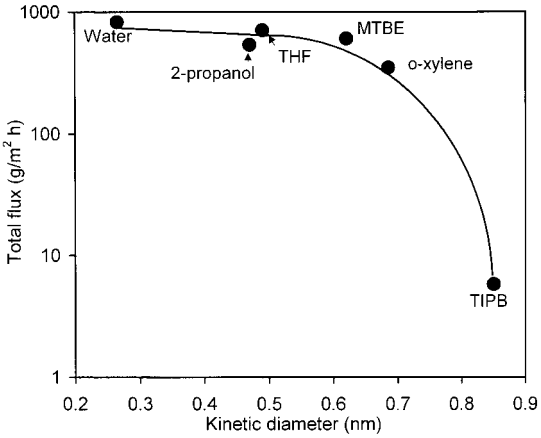

Figure 3. Pervaporation fluxes of pure components at 303 K as a function of kinetic diameter for a beta membrane M2 on a stainless steel support.

Table 1. Pervaporation through a Beta Membrane for Water/Organic Mixtures at 303 K

feed mixture	water feed concn (wt %)	total flux (kg/m²·h)	water permeate concn (wt %)	water/organic separation selectivity
water/THF	6.7	0.74	35	7.5
water/2-propanol	10	0.66	52	10
water/*tert*-butyl alcohol	8	0.60	34	6.0

Single-gas permeances measured at 473 K through the membrane M2 were 9.2×10^{-7} (H_2), 3.0×10^{-7} (N_2), 2.8×10^{-7} (n-C_4), and 2.3×10^{-7} (i-C_4) mol/m²·s·Pa. These permeances are reproducible to within 2% of their values. The ideal selectivities involving H_2 (H_2/N_2, H_2/n-C_4, H_2/i-C_4) are less than the Knudsen selectivities, but Knudsen selectivity is not expected for zeolite pores. Permeances are controlled by both adsorption and diffusion in zeolite pores, and larger molecules have lower diffusivities but higher adsorption coverages than smaller molecules, so the selectivities can be greater than or less than Knudsen. Indeed, the n/i-C_4 ideal selectivity at 473 K was 1.2, which shows that transport is through small pores since the Knudsen selectivity is 1 for isomers. This n-C_4/i-C_4 ideal selectivity is much lower, however, than selectivities obtained on MFI membranes (≈10−20).[15,16] A high n/i-C_4 selectivity is not expected for beta zeolite because both n-C_4 (0.43 nm) and i-C_4 (0.50 nm) are much smaller than the pore size of beta zeolite (0.71 × 0.73 nm), and the diffusivity decreases dramatically as the molecular size approaches the pore size. Light gas permeation is an effective method to evaluate the quality of small- and medium-pore zeolite membranes, but for large-pore zeolite membranes, permeation of larger liquid molecules by pervaporation is a better indication of membrane quality.

(15) Tuan, V. A.; Noble, R. D.; Falconer, J. L. *AIChE J.* **2000**, *46*, 1201.

(16) Tuan, V. A.; Falconer, J. L.; Noble, R. D. *Microporous Mesoporous Mater.* **2000**, *41*, 269.

Table 2. Pervaporation of Mixtures through Large-Pore Membranes at 308 K

membrane (Si/Al ratio)	mixture[a]	total flux (kg/m²·h)	permeate concentration (g/L)		1,3-propanediol/glycerol selectivity
			1,3-propanediol	glycerol	
Y-type (2.5)	ternary	1.6	49	0.058	42
X-type (1.5)	ternary	2.7	30	0.036	41
beta (15)	ternary	1.2	57	0.047	61
beta (15)	binary (1)	1.3	58		
beta (15)	binary (2)	1.5		0.42	

[a] Ternary: 1,3-propanediol/glycerol/water. Binary (1): 1,3-propanediol/water. Binary (2): glycerol/water.

Figure 3 shows that the pervaporation fluxes for pure water (0.265-nm kinetic diameter), tetrahydrofuran (THF, 0.49 nm), 2-propanol (0.47 nm), methyl *tert*-butyl ether (MTBE, 0.62 nm), *o*-xylene (0.685 nm), and triisopropylbenzene (TIPB, 0.85 nm) at 303 K through the beta zeolite membrane M2 decrease with increasing kinetic diameter, except for 2-propanol. Note that TIPB is significantly larger than the beta zeolite pores, and it is expected to permeate only through nonzeolite pores. The TIPB flux of 5.3 g/m²·h indicates that this membrane M2 contains some nonzeolite pores. The other molecules are smaller than the beta pores, and their pervaporation fluxes were ≈2 orders of magnitude higher than the TIPB flux, indicating that the permeation of these molecules was mainly through zeolite pores. The nonzeolite pores are not expected to have high selectivities, so the large difference between water and TIPB permeances indicates that most of the water transport is through the zeolite pores. Thus, the pervaporation results indicate the beta zeolite membranes are of reasonable quality.

Separation of organic/water mixtures by pervaporation was used to evaluate the hydrophilicity/hydrophobicity of the membranes. Organics can be separated from water with hydrophobic membranes, and water can be removed from water/organics mixtures with hydrophilic membranes. We used azeotropic aqueous mixtures with 2-propanol, *tert*-butyl alcohol, and THF as feed since they cannot be separated by conventional distillation.

The pervaporation system was described elsewhere.[17] The membrane had a permeable area of ≈5.2 cm², and the liquid feed (250 cm³) flowed through the inside of the membrane at a flow rate of 20 cm³/s. A liquid nitrogen cold trap condensed the permeate vapor, and permeate samples were weighted to determine the total flux. Permeate concentrations were measured by off-line GC (Hewlett-Packard 5730A) equipped with a 6-ft PORAPAK-Q packed column and a thermal conductivity detector. The composition separation selectivity (α) was calculated as $\alpha_{water/organic} = (y_{water}/y_{organic})/(x_{water}/x_{organic})$, where x and y are the weight fractions in the feed and permeate, respectively.

Table 1 shows that the separation selectivities for the azeotropic mixtures through beta zeolite membrane M2 were 6−10. That is, pervaporation broke the azeotropes. Because water, THF, 2-propanol, and *tert*-butyl alcohol are smaller than the pore size of the beta zeolite, molecular sieving does not control separation. The pure water flux was about 1.2 and 1.5 times the pure THF and 2-propanol fluxes, respectively, but the water/THF and water/2-propanol separation selectivities were higher than these values. That is, water preferentially adsorbed on the membrane and inhibited organic adsorption because the beta membrane is hydrophilic.

Previously, we used a Y-type membrane to separate water from THF.[18] At 303 K and for a 6.7 wt % water feed, the Y-type membrane had a total flux of 0.5 kg/m²·h and a water/THF separation selectivity of 65. Since the Si/Al ratio for the beta zeolite membrane (15) is significantly higher than that for the Y-type membrane (2.5), the beta is less hydrophilic and thus its water/THF separation selectivity is expected to be lower.

The beta zeolite was also used for the separation of 1,3-propanediol ($C_3H_8O_2$, 0.61-nm kinetic diameter) from glycerol ($C_3H_8O_3$, 0.63 nm) by pervaporation. The 1,3-propanediol is an economical source for the production of 3GT (Sorona) polymer, which is a novel polyester with good stretch, recovery, and dyeability. The 1,3-propanediol is obtained by fermentation of glycerol and it must be separated from aqueous glycerol.[19] We have shown previously that large-pore zeolite membranes (X-, Y-, and MOR-types) were effective for 1,3-propanediol separation.[20] The feed concentrations of 1,3-propanediol (100 g/L) and glycerol (5 g/L) were similar to those obtained in industrial fermentation systems. Permeate concentrations were analyzed with a HP 5890 GC equipped with a flame-ionization detector and a 6-ft DB-WAX packed column.

Table 2 compares total pervaporation fluxes, permeate concentrations, and 1,3-propanediol/glycerol separation selectivities with Y- and X-type membranes. The beta membrane had the lowest total flux and the highest 1,3-propanediol permeate concentration. This higher 1,3-propanediol permeate concentration might be expected because the hydrophobicity of the zeolites increased in the order of X < Y < beta. Note that although the beta membrane had a smaller 1,3-propanediol permeate flux (68 g/m²·h) than the X-type (81 g/m²·h) and Y-type membrane (78 g/m²·h), its 1,3-propanediol/glycerol separation selectivity (61) was significantly higher than that of the X-type (41) and Y-type membranes (42).

To understand separation in the ternary mixture (water/1,3-propanediol/glycerol), pervaporation of binary mixtures (water/1,3-propanediol and water/glycerol) was investigated. At 308 K, the 1,3-propanediol permeate concentrations were almost the same for binary and ternary feeds. However, the glycerol permeate concentration for the binary solution was ≈8 times higher than that of the ternary solution. Both 1,3-propanediol and

(17) Liu, Q.; Noble, R. D.; Falconer, J. L.; Funke, H. H. *J. Membr. Sci.* **1996**, *117*, 163.

(18) Li, S.; Tuan, V. A.; Noble, R. D.; Falconer, J. L. *Ind. Chem. Eng. Res.* **2001**, *40*, 4577.

(19) Li, S.; Tuan, V. A.; Falconer, J. L.; Noble, R. D. *J. Membr. Sci.* **2001**, *191*, 53.

(20) Li, S.; Tuan, V. A.; Falconer, J. L.; Noble, R. D. *Chem. Mater.* **2001**, *13*, 1865.

glycerol molecules are smaller than the beta zeolite pores, and thus their permeation is expected to be mainly through zeolite pores. The presence of 1,3-propanediol decreased the glycerol flux, indicating that the separation mechanism of 1,3-propanediol/glycerol through the beta membrane is mainly due to preferential adsorption of 1,3-propanediol.

In summary, pure and highly crystalline beta zeolite membranes were successfully prepared with good reproducibility by in situ crystallization on porous stainless steel tubes. These membranes had good separation selectivity for several organic/water mixtures,

Acknowledgment. We acknowledge support by the University of Colorado and MemPro Corporation.

CM010413E